Identification of the Workspace Boundary Of a General 3-R Manipulator

Erika Ottaviano**, Manfred Husty*, Marco Ceccarelli**

**LARM Laboratory of Robotics and Mechatronics
DiMSAT – University of Cassino
Via Di Biasio 43 - 03043 Cassino (Fr), Italy,
E-mail: ottaviano/ceccarelli@unicas.it

* Institute for Engineering Mathematics Geometry and
Computer Science – University of Innsbruck
Technikerstr. 13 A-6020 Innsbruck, Austria
E-mail: manfred.husty@uibk.ac.at

Keywords: Kinematics, Serial Manipulators, Workspace, Geometric Singularities, Void.

Abstract

In this paper an algebraic formulation is presented for the boundary workspace of 3-R manipulators in Cartesian Space. It is shown that the cross-section boundary curve can be described by a 16-th order polynomial as function of radial and axial reaches. The cross-section boundary curve and workspace boundary surface are fully cyclic. Geometric singularities of the curve are identified and characterized. Numerical examples are presented to show the usefulness of the proposed investigation and to classify the design characteristics.

1. Introduction

Workspace and singularity analyses of serial manipulators have been the focus of intense research in past decades. The computation of the workspace and its boundary is of significant interest because of their impact on manipulator design, placement in a working environment, and trajectory planning.

Most of the industrial manipulators are wrist-partitioned, that is a concatenation of a 3-R (Revolute) arm, i.e., regional structure, and a spherical wrist attached to the terminal link of the arm. The workspace analysis of such manipulator can be performed by considering the

positioning and orienting singularities separately.

Early studies on the subject were developed in (Roth 1975). The relationship between kinematic geometry and manipulator performances has been formulated in (Kumar and Waldron 1981). Gupta and Roth analyzed the effect of hand size on workspace in (Gupta and Roth 1982). An algorithm for the workspace determination of a general N-R robot has been developed in (Tsai and Soni 1983). An algebraic formulation for determining the workspace of 3-R manipulators has been presented in (Ceccarelli 1989) and then generalized for N-R manipulators in (Ceccarelli 1996). Furthermore, the proposed formulation has been used for design purposes in (Ceccarelli 1995), and optimal design procedure in (Lanni et al. 2002; Ceccarelli and Lanni 2004). Numerical criteria to analyze the workspace of a general multi-degree-of-freedom (DOF) system has been formulated in (Haug et al. 1994), based on the study of a row-rank deficiency of its Jacobian. Most of the work has been done on 3-R manipulators for either positioning (Freudenstein and Primrose 1984; Spanos and Kohli 1985), or orienting tasks (Angeles 1988).

The determination of the workspace boundary in Cartesian Space has been attempted also in (Spanos and Kohli 1985; Hsu and Kohli 1987; Smith and Lipkin 1993; Ranjbaran et al. 1992). In (Ceccarelli and Vinciguerra 1995) an analysis of the workspace boundary of 4-R serial manipulator has been studied by employing toroidal geometries and providing algebraic expression. Other papers are related to the singularity of the Jacobian matrix that is usually expressed in the Joint-Coordinate Space. Regions that are free of singularities in the Joint Space have been named C-sheets, (Burdick 1995). In C-sheets it is possible to change posture without passing through singularities (Parenti-Castelli and Innocenti 1988). Manipulators that can change posture without meeting a singularity have been named cuspidal manipulators in (Wenger, 2000) because of the existence of cusps in their workspace.

A method has been introduced in (Wenger 1992) to obtain the separating surfaces. Manipulators that can change posture without meeting a singularity have been named cuspidal manipulators in (Wenger, 2000). A formulation to obtain the boundary of all surfaces enveloping the workspace

for general 3-DOF mechanisms was discussed in (Abdel-Malek and Yeh 1997), although it was already proposed in (Ceccarelli 1989). A formulation has been introduced in (Abdel-Malek and Yeh 1997), for the determination of voids in the workspace of serial manipulators. Furthermore, it has been shown in (Wenger 2000) how to take into account in the design stage the possibility for a manipulator to execute non-singular changing posture motions.

Although there are many reports in the field of the workspace analysis, there are still open problems in the characterization of the workspace boundary. It is of practical interest to detect the presence of a void in the workspace, since it is a region of unreachable points for the end-effector of the manipulator. A ring void is a void that is buried within the workspace volume and has ring topology, (Ceccarelli 1996). The presence of cusps and void can be detected by analyzing the geometric singularities of the cross-section boundary curve (Ottaviano et al. 1999). By analyzing the workspace boundary it has been found that four types of ring voids and eight types of internal branch envelopes may exist. A preliminary classification of ring void types and geometric singularities has been presented in (Ottaviano et al. 1999). Analysis of cusps in the workspace boundary has been proposed also in (Burdick, 1995; Saramago et al., 2002).

The analysis of the internal branch of the cross-section boundary curve leads to a classification to characterize the i-solution region (i=0,2,4) for the Inverse Kinematics Problem (IKP). Furthermore, it is of practical interest exploring the possibility of changing posture without meeting a singularity (Parenti-Castelli and Innocenti 1988). A manipulator is said to change posture if it goes from one inverse kinematic solution to another (Wenger 1992). Changing posture can be desired for obstacle avoidance or to take into account joint limits. Usually, a non-redundant manipulator crosses a singularity when changing posture. A class of manipulator can change posture without meeting a singularity. 3-R manipulators have at most 4 Inverse Kinematic solutions in their workspace. In general, the number of solutions of the IKP varies from one point to another in the workspace, which may include regions with 0, 2, or 4 solutions (Ceccarelli 1995; Wenger 1998). Indeed, a 3R manipulator can be classified as binary or

quaternary, i.e. it may have at most 2 solutions for the IKP, or at most 4 solutions for the IKP (Wenger et al. 2005).

The presence of cusps and void can be detected by analyzing singular points of the curve describing the boundary. Preliminary analyses of geometric singularities of the cross-section boundary curve have been carried out in (Saramago et al. 2002), but to the authors' knowledge in the literature there is not an investigation on singular points of the boundary curve for a general 3-R manipulator. A classification of the singularities for a special class of 3-R manipulator is reported in (Wenger et al. 2005).

The proposed analysis of geometric singularities of a general 3-R manipulator can provide useful tools in the design stage or use. Singular points of the cross-section curve describing the boundary workspace are named characteristic points.

In this paper a Cartesian representation of the workspace boundary of a general 3-R manipulator is presented. Geometric singularities have been determined and used to classify the workspace boundary of the manipulator, and detect the presence of a void. The curve describing the workspace boundary gives also useful information for characterization in Cartesian Space of the i-solution regions (i=0,2,4) for the IKP. Furthermore, the proposed analysis can be used for design purposes and calculation of the workspace volume of the manipulator.

2. An Algebraic Formulation for the Workspace Boundary of 3R Manipulators

A general 3-R manipulator is sketched in Fig.1, in which the kinematic parameters are denoted by the standard Hartenberg and Denavit (H-D) notation. Without loss of generality the base frame is assumed to be coincident with $X_1Y_1Z_1$ frame when $\theta_1= 0$, $a_0=0$ and $d_1=0$. End-effector point H is placed on the X_3 axis at a distance a_3 from O_3, as shown in Fig.1. The general 3R manipulator is described by the H-D parameters a_1, a_2, d_2, d_3, α_1 and α_2, and θ_i, for (i = 1,…,3), as shown in Fig.1. r is the radial distance of point H from the Z_1-axis and z is the axial reach; both can be expressed as function of H-D parameters.

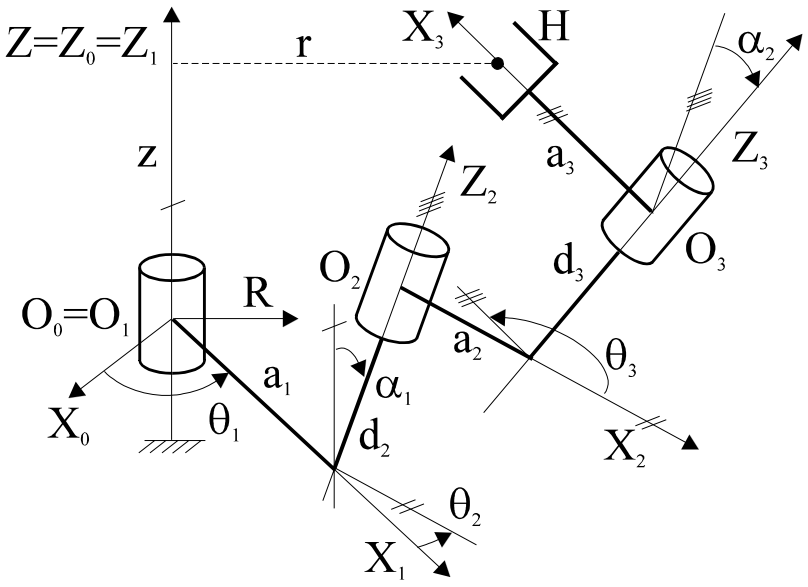

Figure1. Kinematic scheme of a 3R manipulator.

The position workspace of the 3R manipulator can be obtained by a θ_1 rotation of the generating torus that is traced by H by full revolution of θ_2 and θ_3.

Alternatively, the boundary of the position workspace can be determined by considering the envelope surface of the torus family that is traced as function of θ_3, when a torus of the family is obtained by full revolution of θ_1 and θ_2, as outlined in (Ceccarelli 1989, and 1996). In this case, the equation of the workspace boundary of point H can be expressed in the cross-section plane R-Z of the base frame when $\alpha_1 \neq 0$, $C \neq 0$ and $E \neq 0$, in the form of so-called ring equation (Ceccarelli 1989, 1996),

$$z = \frac{-L \pm Q^{1/2}}{KC} - \frac{D}{C}, \qquad r = \left[A - z^2 + \frac{(Cz + D)G + F}{E} \right]^{1/2} \tag{1}$$

in which A, B, C, D, E, F and G are named as architecture coefficients.

The sign ambiguity in z expression can be solved to give two envelope branches that together

give the envelope of the torus family.

Architecture coefficients are function of H-D parameters in the form

$$A = a_1^2 + r_2 + \left(z_2 + d_2\right)^2, \quad B = -4a_2^2 r_2, \quad C = \frac{2a_1}{s\alpha_1}, \quad D = -2a_1\left(z_2 + d_2\right)\frac{c\alpha_1}{s\alpha_1}$$

$$E = -2a_3\left(a_2 s\theta_3 + d_2 s\alpha_2 c\theta_3\right), \quad F = 4a_1^2 a_3\left(a_2 s\theta_3 + a_3 s\theta_3 c\theta_3 \left(s\alpha_2\right)^2 - d_3 c\alpha_2 s\alpha_2 c\theta_3\right) \qquad (2)$$

$$G = \frac{2a_1 a_3 c\theta_3 s\alpha_2 c\alpha_1}{s\alpha_1}, \quad L = FG, \quad K = G^2 + E^2, \quad Q = L^2 - K\left(F^2 + BE^2\right)$$

in which

$$r_2 = \left(a_3 c\theta_3 + a_2\right)^2 + \left(a_3 s\theta_3 c\alpha_2 + d_3 s\alpha_2\right)^2, \; z_2 = d_3 c\alpha_2 - a_3 s\theta_3 s\alpha_2 \qquad (3)$$

The cross-section boundary curve f of the 3-R manipulator workspace in R-Z plane can be thought as the envelope of the θ_3-family curves.

A generating torus of the enveloping θ_3-family can be expressed as

$$\left(r^2 + z^2 - A\right)^2 + \left(Cz + D\right)^2 + B = 0 \qquad (4)$$

In order to obtain a closed-form expression in r and z coordinates from the ring equation (1), one can manipulate Eq. (4) by performing the half-tangent substitution u= tan (θ_3/2) in the form

$$k_4 u^4 + k_3 u^3 + k_2 u^2 + k_1 u + k_0 = 0 \qquad (5)$$

Parameters k_i (i = 0,…,4) of Eq. (5) are functions of the H-D parameters, z and r. They can be expressed in the form

$$k_i = K_{iR4}\, r^4 + K_{iR2}\, r^2 + K_{iR0} + K_{iZ4}\, z^4 + K_{iZ2}\, z^2 + K_{iR2Z2}\, r^2 z^2 + K_{iZ1}\, z \qquad (6)$$

As the coefficients k_i are functions of the r and z parameters, Eq. (5) represents a one-parameter family of curves. The envelope of this family is obtained by eliminating u from Eq. (5) and its derivatives with respect u. This yields to the function f expressing the cross-section boundary curve in the form

$$f = \sum_{i=0}^{8} c_i \left(r^2 + z^2\right)^i + \sum_{j=0}^{7} c_{bj}\, z \left(r^2 + z^2\right)^j \qquad (7)$$

Coefficients c_i and c_{bj} are non-linear expressions of the H-D parameters and can be obtained by K_{iRj} K_{iRjZj} and K_{iZj} coefficients in Eq. (6) together with Eqs. (2-3). For example, c_8 coefficient can be expressed as

$$c_8 = 65{,}536\, a_3^4 a_1^4 (s\alpha_1)^8 (s\alpha_2)^4 \qquad (8)$$

Equation (7) represents the Cartesian expression in R-Z coordinates for the cross-section boundary curve for a general 3-R manipulator. Its expression is function of the H-D parameters through c_i and c_{bj} coefficients. This expression can be used to characterize the workspace boundary better than using Eq. (1).

3. Characteristics of the Cross-Section Boundary Curve

The cross-section boundary curve f in Eq. (7) is fully cyclic and of 16-th degree; it has 2 singular points at infinity with multiplicity 8 each, that are the 2 circle points. A curve that has the imaginary circular points as double, triple, points is said to have circularity 2, 3, (Hunt 1978;

Naas at al. 1974). Therefore, the cross-section boundary curve has circularity 8.

A descriptive proof is reported in Fig.2, which shows the cross-section boundary curve as an envelope with an inner branch, which may give the boundary of a ring void, and an outer branch, which represents the boundary of the bulk workspace ring.

The boundary surface of the 3R manipulator workspace is fully cyclic too and its degree is 16 yet. This can be proved since r^2 in Eq.(7) is expressed as (x^2+y^2), in which x and y are components of the position vector of point H with respect to the base frame. Furthermore, f is symmetric with respect to the Z axis. This can be proved since Eq. (7) contains only even powers of r. The degree of the curve does not change under rotation because of its symmetry and partial derivatives.

By analyzing the polynomial expression of Eq. (7), it has been found that the degree of the cross-section boundary curve is lower than 16 iff:

– $a_3=0$. The polynomial expression (7) is not valid since the formulation implies that $E\neq 0$. This occurrence refers to the design case in which the operation point H coincides with the origin O_3 of the $X_3Y_3Z_3$ reference frame. In such case the θ_3 rotation has no effect on the workspace and the ring workspace degenerates in a 2R chain workspace.

– $\alpha_1=0$. The polynomial expression (7) is not valid since the formulation implies that $\alpha_1\neq 0$.

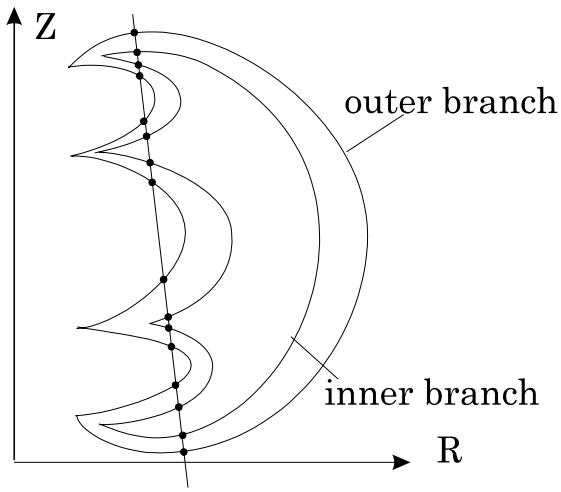

Figure2. A descriptive proof of the 16th degree of the cross-section boundary.

– α_2=0. This occurrence refers to the design case in which Z_2 and Z_3 axes are parallel. The outcome of a Maple computation is that the cross-section boundary curve is of degree 12.

- a_1=0. The polynomial expression (7) is not valid since the formulation implies that C≠0.

By analyzing Eq. (8) one can also note that c_8 coefficient, that gives the full degree of the curve, does not depend on a_2, d_2 and d_3 parameters.

4. A Classification of the Geometric Singularities

In general, a singularity is a point at which an equation, curve, or surface, becomes degenerate. Singularities are often also called singular points or geometric singularities (Gibson, 1998).

Singularities are extremely important in complex analysis, because they characterize all possible behaviors of analytic functions. Complex singularities are points in the domain of a function where the function fails to be analytic. Isolated singularities may be classified as poles, essential singularities, logarithmic singularities, or removable singularities. Non-isolated singularities may arise as natural boundaries or branch cuts.

Real geometric singularities of the cross-section boundary curve f can be found by introducing the homogeneous coordinate w in Eq. (7). Thus, one can consider this new equation, which is function of r, z and w, together with its partial derivatives f_r f_z and f_w with respect to r, z, and w, respectively.

The zeros of the set of equations: $f = 0$; $f_r = 0$; $f_z = 0$; and $f_w = 0$ gives the geometric singularities of the cross-section boundary curve f. Points belonging to these zeros are denoted by C_i, D_i, and A_i where C_i indicates cusps, D_i double points and A_i acnodes, referring to a geometric interpretation that is shown in Fig. 3. They can be classified by considering the second partial derivatives of f in the form (Gibson, 1998)

$$g = f_{rz}^2 - f_{rr} f_{zz} \tag{9}$$

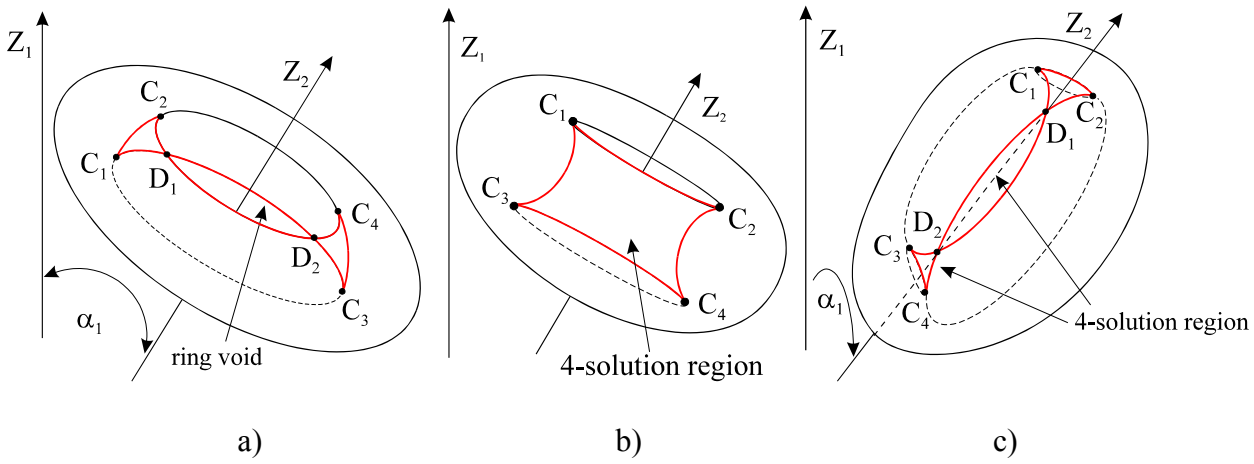

Figure 3. The generating manifold for the workspace with characteristic points:

a) a general case; b) a cuspidal manipulator; c) manipulator with double points but no void.

Functions g, f_r, f_z, and f_w can be useful to fully characterize real geometric singularities in the workspace of the 3R manipulators.

A point D_i, whose coordinates are (rd_i,zd_i), is a double point iff Eq. (9) is greater than zero. A point C_i, whose coordinates are (rc_i,zc_i), is a cusp iff Eq. (9) is equal to zero. A point A_i, whose coordinates are (ra_i,za_i), is an acnode iff Eq. (9) is less than zero.

A condition on Eq. (9) is useful to characterize the cross-section boundary curve and ring void of the workspace of 3R manipulators through the points whose geometrical classification is shown in Fig. 3.

The relationships between the number of singularities of planar algebraic curves is given by the Pucker's equations (Husty et al. 1997) whose counting can be expressed in the form

$$\begin{aligned} m &= n(n-1) - 2\delta - 3\kappa \\ \kappa &= 3m(m-2) - 6\tau - 8\iota \\ n &= m(m-1) - 2\tau - 3\iota \\ i &= 3n(n-2) - 6\tau - 8\kappa \end{aligned} \qquad (10)$$

where m is the class, n the curve order, δ the number of ordinary double points, κ the number of cusps, ι the number of stationary tangents (inflection points), and τ the number of bi-tangents. Only three of (10) are linearly independent. Equations (10) can give a complete classification of all singular points of the cross-section boundary curve in Eq. (7).

A point D_i is an ordinary double point if its pre-image under f consists of two values and the two tangent vectors are non-collinear. Geometrically, the meaning is that in a neighborhood of D_i, the curve consists of two transverse branches, as shown in Fig.3a).

A cusp point C_i is a point at which two branches of a curve meet such that the tangents of each branch are equal, as shown in Fig.3b). An inflection point is a point on a curve at which the sign of the curvature (i.e., the concavity) changes. A bi-tangent is a line that is tangent to a curve at two distinct points. An isolated point on a curve A_i, also known as an acnode or hermit point is a point which has no other points in its neighborhood. Furthermore, the cross-section boundary curve, as composed by internal and external branches, can be classified into two classes: with intersecting and non-intersecting branches. For the second class a classification of possible types of ring void has been presented in a preliminary view in (Ottaviano et al., 1999), in which it has been pointed out the presence and importance of double points in the cross-section boundary curve. Examples in Fig. 3 explain the topology of the possible types of internal branches that are reported as a complete classification in Fig. 4. Geometric singularities of the cross-section boundary curve can be identified as double points D_i, acnodes A_i and cusp points C_i. Internal branch of the boundary envelope curve in the cross section in R-Z shows generally three loops. The middle loop can delimit the ring void or a 4-solution region and it is a part of the boundary curve as pointed out in (Ceccarelli 1989); the others are related to 4-solution regions for the Inverse Kinematics problem. A ring void can be characterized by the presence of double points, which have been named as D_1 and D_2 in Fig. 3. Points D_1 and D_2 are double points, i.e. intersections of the inner branch. If there are no double points but there are cusps there is not a void inside the workspace. In this case, the manipulator belongs to the class of the cuspidal

manipulators, Fig.3b). Double points may indicate the presence of a void that corresponds to a 0-solution region for the Inverse Kinematics problem. Cusp points C_1 to C_4 can be considered characteristic points for the cross-section boundary curve since they delimit workspace regions with multiple configuration reachability. The presence of double points and acnodes, as shown in Fig. 4, indicates the presence of 4 solution regions for the Inverse Kinematic problem. Acnodes in Fig. 4 denote the presence of regions with 4-solutions for the IKP. Manipulators with acnodes present only 2 types of regions: 2 and 4 solution regions. Figure 4 shows a classification in which there are inner branches that give a ring void and inner branches that indicates the presence of 4-solution region for the Inverse Kinematic problem. Regions can be suitably classified by considering a check on the number of possible solutions for the IKP.

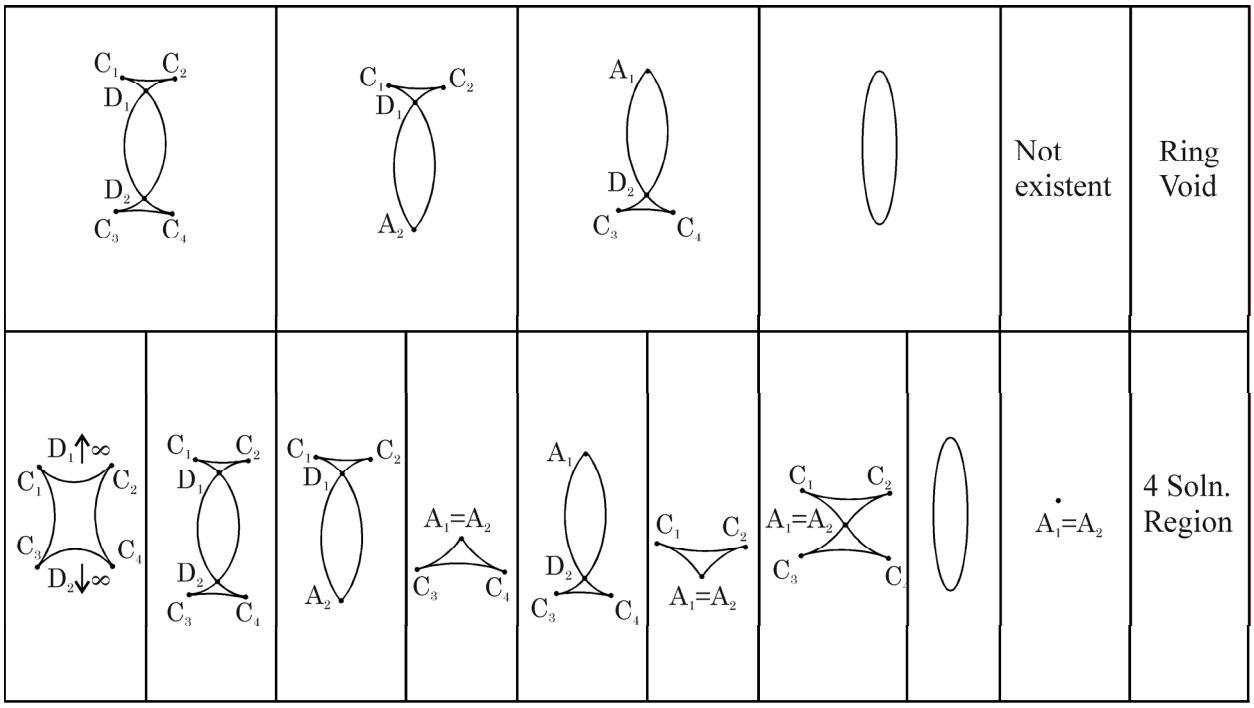

Figure 4. Manifolds for inner branches of the workspace boundary envelope of 3R manipulators.

5. Numerical examples

Numerical examples are reported to show most significant cases in the classification of Fig. 4.

Geometric singularities have been determined for all the reported examples as zeros set of equations: $f = 0$; $f_r = 0$; $f_z = 0$; and $f_w = 0$; and classified through Eq. (9). It is worth to note that singular point coordinates will be reported with few decimals, but for their determination and classification 50 digits have been used in Maple computation.

Figure 5a) shows the cross-section boundary curve of a general case like in Fig. 3. The inner loop is characterized by the presence of 2 double points and represents a void. Other 2 loops that are characterized by the cusps are reachable regions of the workspace. Figure5b) shows a plot of the boundary curve together with f derivatives. It is possible to observe that the derivatives f_r, f_z, and f_w of the cross-section boundary curve meet at the three singular points D_1, C_1 and C_2. Their coordinates can be computed as the zeros of the set of the f derivatives. Their coordinates are: D_1=[3.82, 6.62]; C_1=[1.87, 7.12]; C_2=[3.09, 7.16]. The nature of those characteristic points has been checked by Eq. (9). It has been verified that C_1 and C_2 are cusps, since g is equal to zero, and D_1 is a double point, since g is greater than zero.

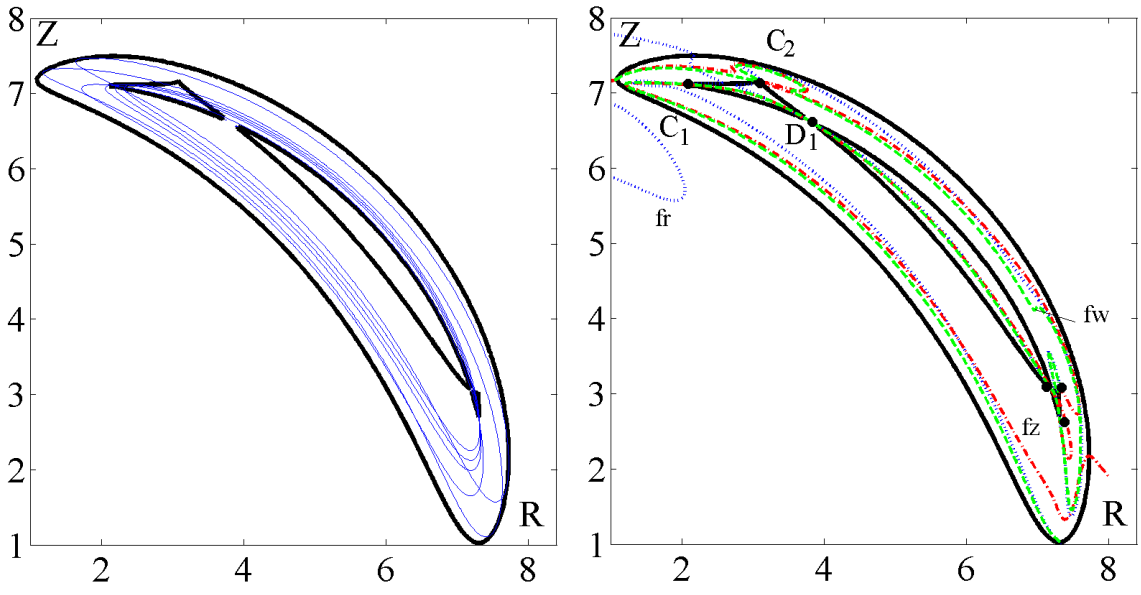

Figure 5. A numerical example for a 3R manipulator with a_1=1u; a_2=1u; a_3=1u; d_2=3u; d_3=5u; $\alpha_1=\pi/4$; $\alpha_2=\pi/4$: a) cross-section boundary curve f and curves of the 1-parameter family; b) f, f_r , f_z, f_w plots. (u is the unit length, and angles are expressed in radians)

In Fig.6 the workspace boundary of a cuspidal manipulator is shown. Points C_1=[1.87, 4.13]; C_2=[2.99, 4.25], C_3=[4.36, 2.07]; C_4=[4.38, 2.89] have been checked through Eq. (9).

Figure 7 shows a numerical example in which the cross-section boundary curve f contains only even powers of r and z. The cross-section boundary curve is of 16^{th} order. There are no cusps nor double points, no voids, but the internal envelope branch individuates 4-solution region only. Points A=[1.21, 0.00] and A_2=[1.36, 0.00] are acnodes, since g is less than zero. The manipulator in the numerical example of Fig. 7 is a quaternary manipulator (Wenger et al. 2005).

Figure 8 shows a numerical example in which the cross-section boundary curve has not only even powers of z. Coordinates of the three singular points on the inner branch are: C_1=[1.28, 0.09]; A_1=[3.35, 2.5]; C_2=[4.60, 0.36]. By evaluating Eq.(9) at points C_1, C_2 and A_1 it has been verified that C_1 and C_2 are cusps, since the function g is equal to zero, and A_1 is an acnode, since g is less than zero. Therefore, the presence of an acnode on the inner branch denotes the existence of a 4-solution region for the Inverse Kinematic problem.

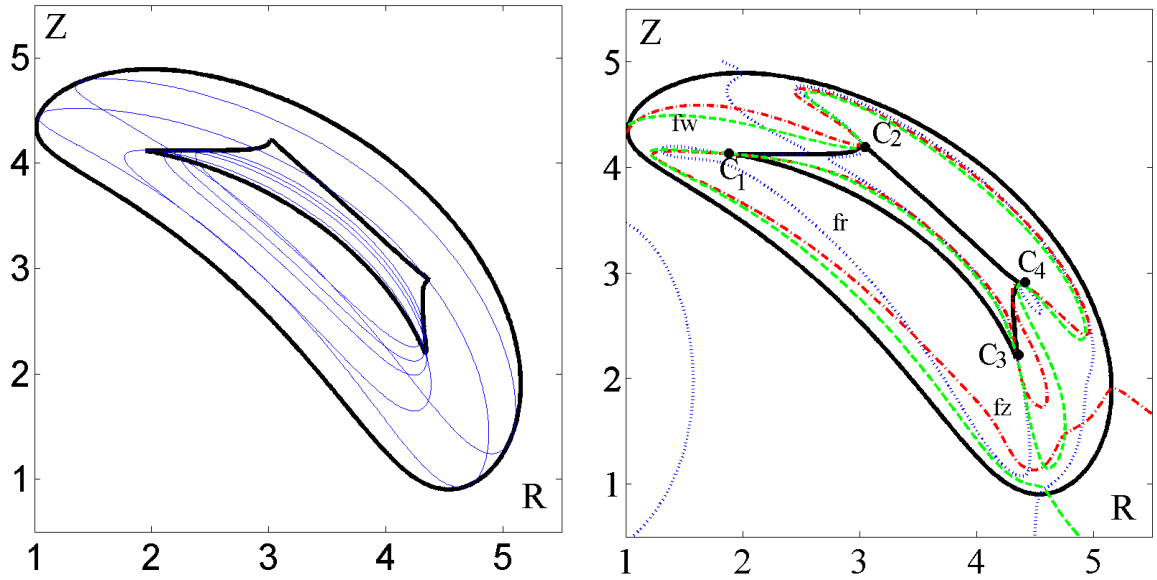

a) b)

Figure 6. A numerical example for a 3R manipulator with a_1=1u; a_2=1u; a_3=1u; d_2=3u; d_3=2u; $\alpha_1=\pi/4$; $\alpha_2=\pi/4$: a) cross-section boundary curve f and curves of the 1-parameter family; b) f, f_r, f_z, f_w plots.(u is the unit length, and angles are expressed in radians)

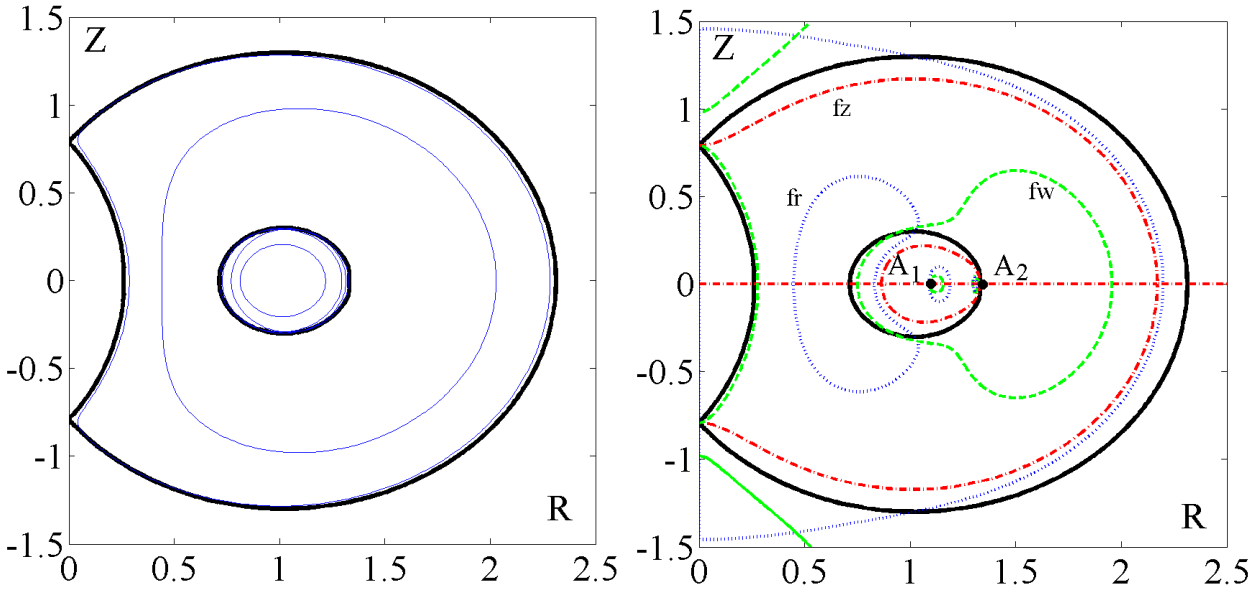

a) b)

Figure 7. A numerical example for a 3R manipulator with a_1=1u; a_2=0.5u; a_3=0.8u; d_2=0.2u; d_3=0; α_1=-π/2; α_2=π/2: a) cross-section boundary curve f and curves of the 1-parameter family; b) f, f_r , f_z, f_w plots. (u is the unit length, angles are expressed in radians)

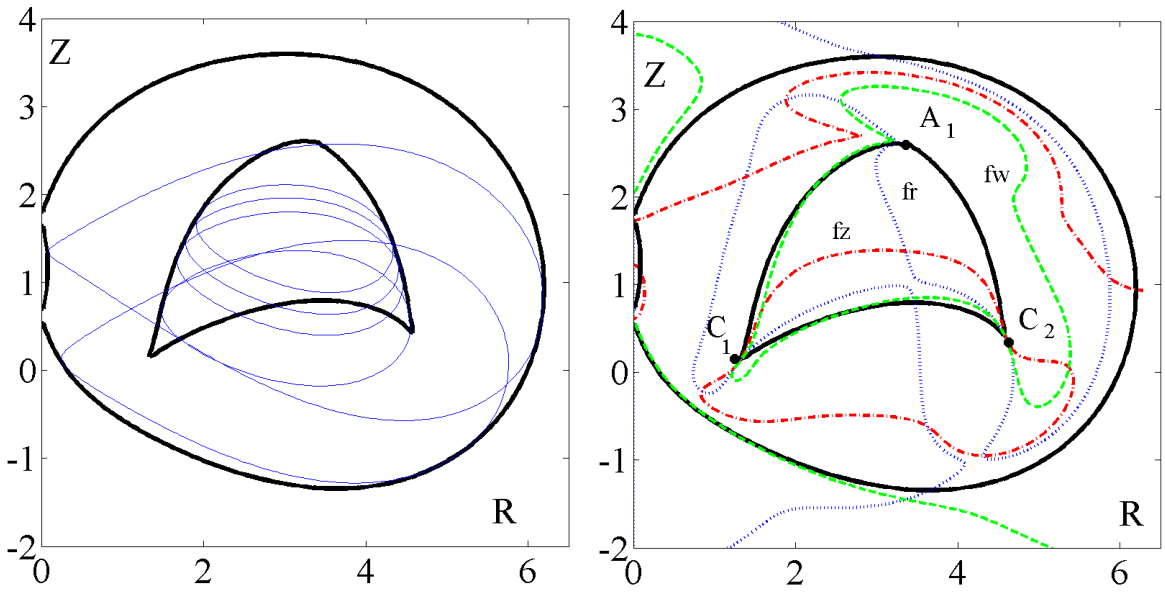

a) b)

Figure 8. A numerical example for a 3R manipulator with a_1=3u; a_2=1u; a_3=3u; d_2=1u; d_3=1u; α_1=-π/6; α_2=π/3: a) cross-section boundary curve f and curves of the 1-parameter family; b) f, f_r, f_z, f_w plots. (u is the unit length, angles are expressed in radians)

Figure 9 shows a numerical example in which the algebraic expression of the boundary curve has the degree of 16. The computation shows that the cross-section boundary curve does not contain singular points, as it is shown in Fig. 9b) in which f_r, f_z and f_w do not intersect. The manipulator is a binary manipulator (Wenger et al. 2005) since the presence of 2 solution region for the IKP.

The numerical example of Fig. 10 shows that the cross-section boundary curve has only even powers of r and z and the degree of the curve is 16. Singular points have coordinates: A_1=[0.97, 0.00]; D_1=[5.73, 0.00]; C_1=[6.87, -3.72]; C_2=[6.87, 3.72]. A_1 has g less than zero (acnode), D_1 has g grater than zero (double point) and C_1 and C_2 have g equal to zero (cusps). It is worth to note that in this case internal branches delimit two 4-solution regions for the IKP.

Numerical example of Fig. 11 shows a cross-section boundary curve of 16th degree. Singular points that have been checked are C_1=[1.64, 2.77]; D_1=[1.85, 2.56]; C_2=[1.11, 2.70] and A_1=[3.03, 1.51]. It can be proved that C_1 and C_2 are cusps, since function g at those points has value equal to zero.

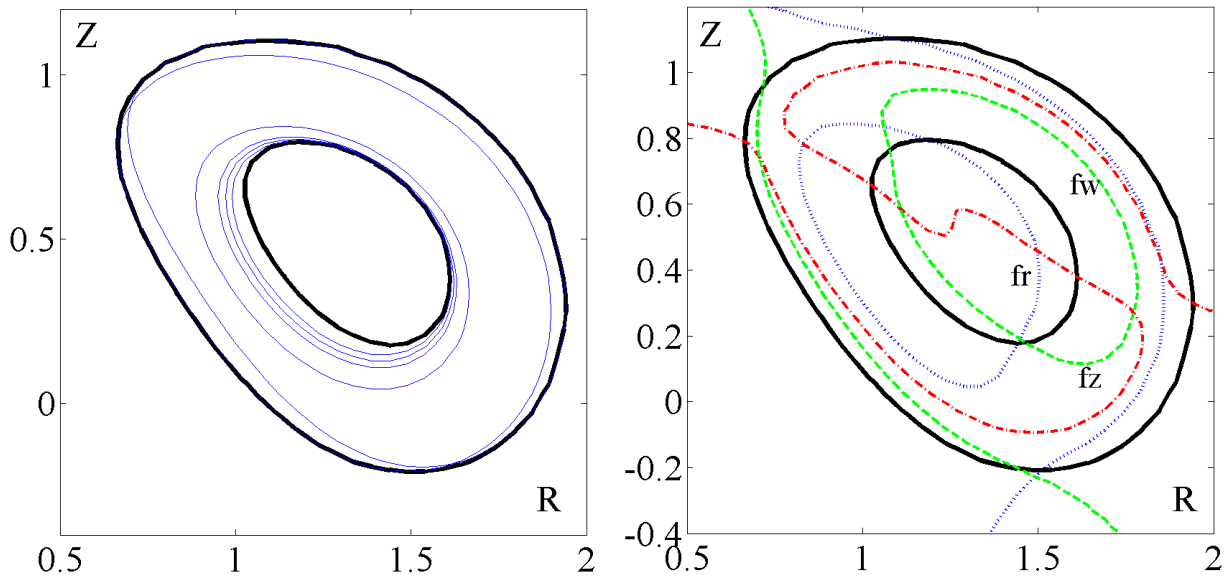

Figure 9. A numerical example for a 3R manipulator with a_1=1u; a_2=0.5u; a_3=0.2u; d_2=0.5u; d_3=0.5; $\alpha_1=\pi/3$; $\alpha_2=\pi/6$: a) cross-section boundary curve f and curves of the 1-parameter family; b) f, f_r, f_z, f_w plots. (u is the unit length, angles are expressed in radians)

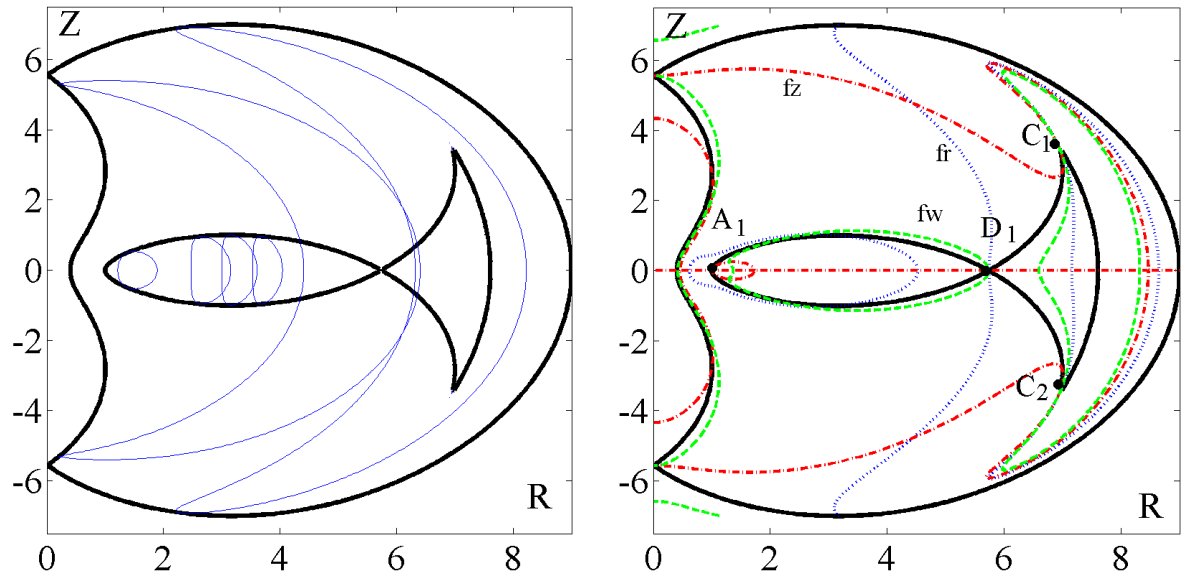

Figure 10. A numerical example for a 3R manipulator with a_1=1u; a_2=3u; a_3=4u; d_2=3u; d_3=0; α_1=-π/2; α_2=π/2: a) cross-section boundary curve f and curves of the 1-parameter family; b) f, f_r, f_z, f_w plots. (u is the unit length, angles are expressed in radians)

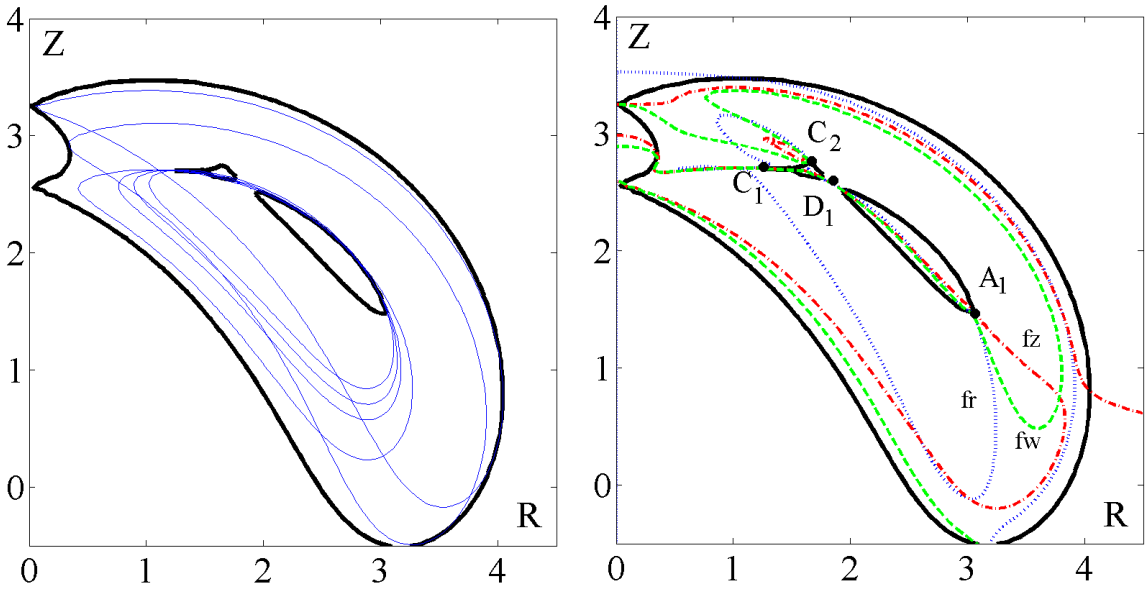

Figure 11. A numerical example for a 3R manipulator with a_1=1u; a_2=1u; a_3=1u; d_2=1u; d_3=2; α_1=π/4; α_2=π/4: a) cross-section boundary curve f and curves of the 1-parameter family; b) f, f_r, f_z, f_w plots. (u is the unit length, angles are expressed in radians)

Point D_1 is a double point since it has g greater than zero and A_1 is an acnode, since g is less than zero. It indicates the presence of a void. The inner branch of the cross-section boundary curve delimits a void and one 4-solution region for the IKP.

Figure 12 shows a cross-section boundary curve that contains only even powers of z. In this numerical example inner and outer branches of the cross-section boundary curve intersect. The degree of the curve is 16. Singular points that have been checked are C_1=[4.42, 0.96]; D_1=[4.92, 2.69]; C_2=[6.68, 3.56]. It can be proved that C_1 and C_2 are cusps, since by evaluating g at those points it has values equal to zero. Point D_1 is a double point since it has g greater than zero.

Figure 13 shows a numerical example for an industrial robot Mitsubishi MRP-700A. It is worth noting that the resulting workspace boundary has been obtained without considering joint limits. The manipulator under study belongs to a special case, in which α_2 is equal to zero. As expected, the polynomial expression for the workspace boundary is of 12^{th} order. There no geometric singularities. The manipulator has no void and a 4-solution region.

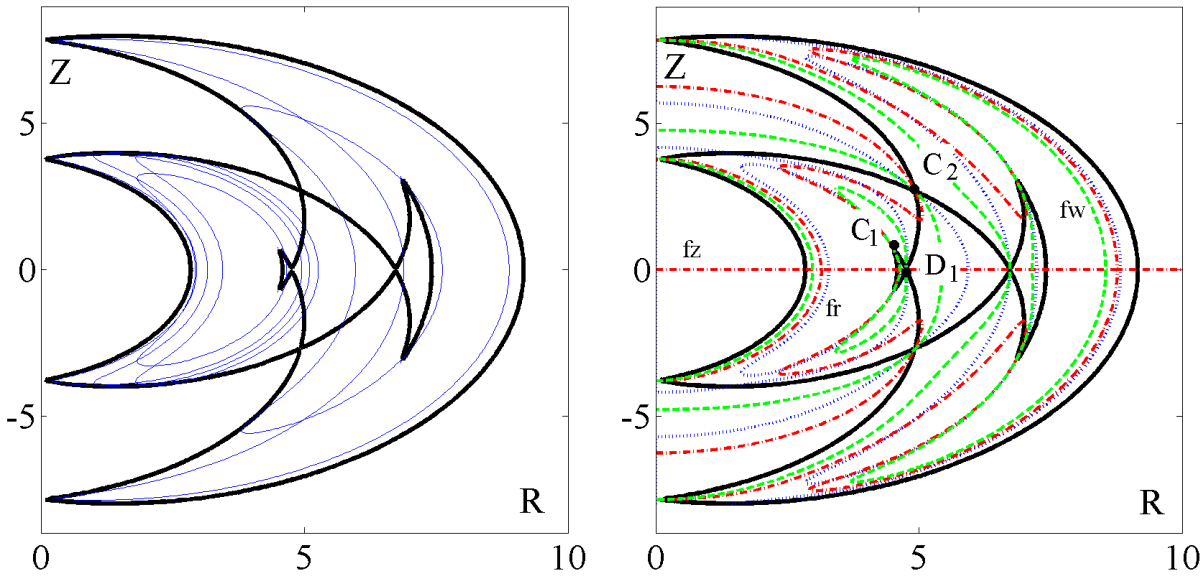

Figure 12. A numerical example for a 3R manipulator with a_1=1u; a_2=2u; a_3=6u; d_2=1u; d_3=0; α_1=-π/2; α_2=π/2: a) cross-section boundary curve f and curves of the 1-parameter family; b) f, f_r, f_z, f_w plots. (u is the unit length, angles are expressed in radians)

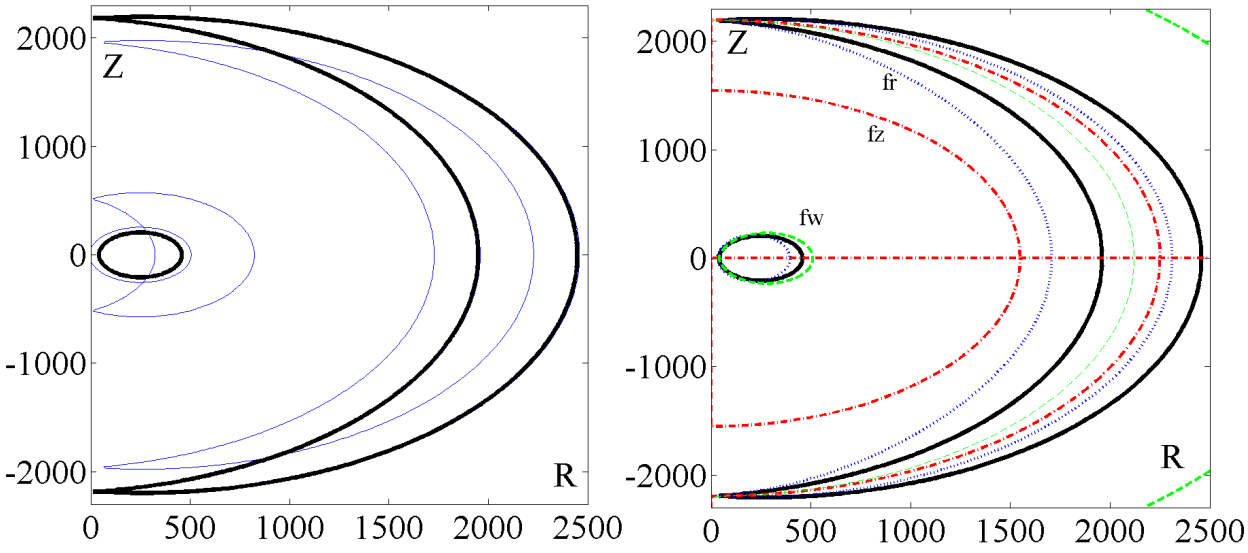

a) b)

Figure 13. A numerical example for Mitsubishi MRP-700A manipulator with a_1=250; a_2=1000; a_3=1209; d_2=0; d_3=0; $\alpha_1=\pi/2$; α_2=0: a) cross-section boundary curve f and curves of the 1-parameter family; b) f, f_r, f_z, f_w plots. (lengths are expressed in mm, angles are expressed in radians)

6. Conclusion

An algebraic formulation has been presented for a Cartesian representation of the workspace boundary of a general 3-R manipulator. In particular, with the formulation derived in this paper it is possible to apply the vast geometric literature on algebraic curves to workspace analysis. It has been found that the cross-section boundary curve and boundary surface are of 16-th degree and fully cyclic. Furthermore, a formulation has been presented to identify all geometric singularities of the cross-section boundary curve. Geometric singularities of the cross-section boundary curve are identified as double points, cusps and acnodes, and classified as delimiting ring void and 4-solution regions. Numerical examples have been presented to outline the practical feasibility of the proposed formulation but mainly for a characterization of the manifolds for the inner branch of the workspace boundary envelope. In particular, it is possible to characterize the workspace by analyzing inner braches delimiting 2-solution regions and 4-solution regions for the IKP.

Furthermore, the proposed analysis can be useful for design purposes and to deduce an evaluation of the workspace volume by integrating the boundary curve.

References

Abdel-Malek K., Yeh H-J., 1997, "Analytical Boundary of the Workspace for General 3-DOF Mechanisms", The International Journal of Robotics Research, Vol. 16, No.2, pp. 198-213.

Abdel-Malek K., Yeh H-J., Othman S., 2000, "Understanding Voids in the Workspace of Serial Robot Manipulators", ASME DETC 2000 Biennial Mechanism Conference, Baltimore.

Angeles J., 1988, "Special Loci of the Workspace Spherical Wrists", Proceedings of the First International Workshop on Advances in Robotics Kinematics, Ljubljana, pp. 36-45.

Bruce, J. W., Giblin, P. J., 1992, "Curves and Singularities: A Geometrical Introduction to Singularity Theory", Cambridge University Press, 2nd Edition.

Burdick, J. W., 1995, "A Classification of 3R Regional Manipulator Singularities and Geometries", Mechanism and Machine Theory, Vol. 30, No.1, pp. 71-89.

Ceccarelli M., 1989, "On the Workspace of 3R Robot Arms", Proceedings of the Fifth IFToMM International Symposium on Theory and Practice of Mechanism, Bucharest, Vol. II-1, pp. 37-46.

Ceccarelli M., 1996, "A Formulation for the Workspace Boundary of General N-Revolute Manipulators", Mechanisms and Machine Theory, Vol.31, No.5, pp. 637-646.

Ceccarelli M., Vinciguerra A., 1995, "On the Workspace of General 4R Manipulators", The International Journal of Robotics Research, Vol.14, No.2, pp. 152-160.

Ceccarelli M., Lanni C., 2004, "A Multi-Objective Optimum Design of General 3R Manipulators for Prescribed Workspace Limits", Mechanism and Machine Theory, Vol. 39, pp. 119-132.

Freudenstein F., Primrose E.J.F., 1984, "On the Analysis and Synthesis of the Workspace of a Three-Link, Turning-Pair Connected Robot Arm", ASME Journal of Mechanisms, Transmissions and Automation in Design, Vol.106, pp. 365-370.

Gibson C.G., 1998, “Elementary Geometry of Algebraic Curves”, Cambridge University Press.

Gupta K. C., 1986, “On the Nature of Robot Workspace”, The International Journal of Robotics Research, Vol.5, No.2, pp. 112-121.

Gupta, K. C., Roth, B., 1982, “Design Considerations for Manipulator Workspace”, ASME Journal of Mechanical Design, Vol. 104, pp. 704-711.

Haug E. J., Adkins R., Luh C. M., 1994, “Numerical Algorithms for Mapping Boundaries of Manipulator Workspaces”, Proc. 23rd ASME Mechanisms Conference, Minneapolis.

Hayes M.J.D., Husty M.L., Zsombor-Murray P.J., 2002, “Singular Configurations of Wrist-Partitioned 6R Serial Robots: A Geometric Perspective for Users”, CSME Transactions, Vol. 26, No. 1, 41-55.

Hsu M.S., Kohli D., 1987, “Boundary Surfaces and Accessibility Regions for Regional Structures of Manipulators”, Mechanism and Machine Theory, Vol.22, No.3, pp. 277-289.

Hunt K.H., “Kinematic geometry”, Clarendon Press, Oxford, 1978.

Husty M., Karger A., Sachs H., Steinhilper W., “Kinematik und Robotik“, Springer Verlag, 1997.

Kumar A., Waldron K.J., 1981, “The Workspace of a Mechanical Manipulator”, ASME Journal of Mechanical Design, Vol.103, pp. 665-672.

Lanni C., Saramago S., Ceccarelli M., 2002, "Optimum Design of General 3R Manipulators by Using Traditional and Random Search Optimization Techniques", Journal of the Brazilian Society of Mechanical Sciences, Vol. XXIV, n.4, pp.293-301.

Naas J., Schmidt H.L., “Mathematisches Wörterbuch“, Band II, Akademieverlag Berlin-Teubner Verlag Stuttgart, 1974.

Parenti-Castelli V., Innocenti C., 1988, “Position Analysis of Robot Manipulators: Regions and Sub-Regions”, Proceedings of the First International Conference on Advances in Robot Kinematics, Ljubljana, pp.150-158.

Ranjbaran F., Angeles J., Patel R.V., 1992, “The Determination of the Cartesian Workspace of General Three-Axes Manipulators”, Proceedings of the Third International Workshop on

Advances in Robotics Kinematics, Ferrara, pp. 318-325.

Ottaviano E., Ceccarelli M., Lanni C., 1999, "A Characterization of Ring Void in Workspace of Three-Revolute Manipulators", Proceedings of the Tenth World Congress on the Theory of Machines and Mechanisms, Oulu, Vol.3, pp. 1039-1044.

Ottaviano E., Husty M., Ceccarelli M., 2004, "A Cartesian Representation for the Boundary Workspace of 3R Manipulators", Advances in Robot Kinematics, Ed. Kluwer Academic Publishers, Sestri Levante, pp. 247-254.

Roth B., 1975, "Performance Evaluation of Manipulators from a Kinematic Viewpoint", National Bureau of Standards Special Publication, No. 459, pp. 39-61.

Tsai Y.C., Soni A.H., 1983, "An Algorithm for the Workspace of a General n-R Robot", Journal of Mechanisms, Transmission and Automation in Design, Vol.105, pp. 70-78.

Saramago S., Ottaviano E., Ceccarelli M., 2002, "A Characterization of the Workspace Boundary of Three-Revolute Manipulators", Proceedings of DETC'02 ASME 2002 Biennial Robotics Conference, Montreal, 2002 , paper DETC2002/MECH-34342.

Smith D.R., 1990, "Design of Solvable 6R Manipulators", Ph.D. Thesis, Georgia Institute of Technology, Atlanta.

Smith D.R., Lipkin H., 1993, "Higher Order Singularities of Regional Manipulators", Proceedings of the IEEE International Conference on Robotics and Automation, Vol.1, pp. 194-199.

Spanos J., Kohli D., 1985, "Workspace Analysis of Regional Structures of Manipulators", ASME Journal of Mechanisms, Transmission and Automation in Design, Vol.107, pp. 216-222.

Wenger P., 1992, "A New General Formalism for the Kinematic Analysis of all Nonredundant Manipulators", ", Proc. IEEE International Conference on Robotics and Automation, Nice, Vol.1, pp. 442-447.

Wenger P., 2000, "Some Guidelines for the Kinematic Design of New Manipulators",

Mechanisms and Machine Theory, Vol.35, No.3, pp.437-449.

Wenger P., Chablat D., Baili M., 2005, "A DH Parameter Based Condition for 3R Orthogonal Manipulators to Have Four Distinct Inverse Kinematic Solutions", ASME Journal of Mechanical Design, ,Vol.127, No.1, pp 150-155.

List of Figure Captions

Figure1. Kinematic scheme of a 3R manipulator.

Figure2. A descriptive proof of the 16^{th} degree of the cross-section boundary.

Figure 3. The generating manifold for the workspace with characteristic points: a general case; b) a cuspidal manipulator; c) manipulator with double points but no void.

Figure 4. Manifolds for inner branches of the workspace boundary envelope of 3R manipulators.

Figure 5. A numerical example for a 3R manipulator with a_1=1u; a_2=1u; a_3=1u; d_2=3u; d_3=5u; $\alpha_1=\pi/4$; $\alpha_2=\pi/4$: a) cross-section boundary curve f and curves of the 1-parameter family; b) f, f_r , f_z, f_w plots. (u is the unit length, and angles are expressed in radians)

Figure 6. A numerical example for a 3R manipulator with a_1=1u; a_2=1u; a_3=1u; d_2=3u; d_3=2u; $\alpha_1=\pi/4$; $\alpha_2=\pi/4$: a) cross-section boundary curve f and curves of the 1-parameter family; b) f, f_r, f_z, f_w plots.(u is the unit length, and angles are expressed in radians)

Figure 7. A numerical example for a 3R manipulator with a_1=1u; a_2=0.5u; a_3=0.8u; d_2=0.2u; d_3=0; $\alpha_1=-\pi/2$; $\alpha_2=\pi/2$: a) cross-section boundary curve f and curves of the 1-parameter family; b) f, f_r , f_z, f_w plots. (u is the unit length, angles are expressed in radians)

Figure 8. A numerical example for a 3R manipulator with a_1=3u; a_2=1u; a_3=3u; d_2=1u; d_3=1u; $\alpha_1=-\pi/6$; $\alpha_2=\pi/3$: a) cross-section boundary curve f and curves of the 1-parameter family; b) f, f_r, f_z, f_w plots. (u is the unit length, angles are expressed in radians)

Figure 9. A numerical example for a 3R manipulator with a_1=1u; a_2=0.5u; a_3=0.2u; d_2=0.5u; d_3=0.5; α_1=π/3; α_2=π/6: a) cross-section boundary curve f and curves of the 1-parameter family; b) f, f_r, f_z, f_w plots. (u is the unit length, angles are expressed in radians)

Figure 10. A numerical example for a 3R manipulator with a_1=1u; a_2=3u; a_3=4u; d_2=3u; d_3=0; α_1=-π/2; α_2=π/2: a) cross-section boundary curve f and curves of the 1-parameter family; b) f, f_r, f_z, f_w plots. (u is the unit length, angles are expressed in radians)

Figure 11. A numerical example for a 3R manipulator with a_1=1u; a_2=1u; a_3=1u; d_2=1u; d_3=2; α_1=π/4; α_2=π/4: a) cross-section boundary curve f and curves of the 1-parameter family; b) f, f_r, f_z, f_w plots. (u is the unit length, angles are expressed in radians)

Figure 12. A numerical example for a 3R manipulator with a_1=1u; a_2=2u; a_3=6u; d_2=1u; d_3=0; α_1=-π/2; α_2=π/2: a) cross-section boundary curve f and curves of the 1-parameter family; b) f, f_r, f_z, f_w plots. (u is the unit length, angles are expressed in radians)

Figure 13. A numerical example for Mitsubishi MRP-700A manipulator with a_1=250; a_2=1000; a_3=1209; d_2=0; d_3=0; α_1=π/2; α_2=0: a) cross-section boundary curve f and curves of the 1-parameter family; b) f, f_r, f_z, f_w plots. (lengths are expressed in mm, angles are expressed in radians)